Evaluating Cervical Airbag Effectiveness in Rear and Lateral Impacts to Identify Optimal Pressure for Varying Impact Energies

Ema Jokubaityte, Juan M. Asensio-Gil, Jolyon Carroll, Manuel Valdano, Carlos Rodriguez-Morcillo, Nil Oleaga-Ortega, Lucas Llobet-Cusi, Francisco J. Lopez-Valdes

Abstract Helmets have been developed to mitigate blunt head trauma to cyclists, but other body region injuries have been given less attention, particularly the neck. Initial studies have shown that cervical airbags successfully reduce neck range of motion, associated with cervical spine fragment failure. This work conducts a parametric study with the aim to assess the effectiveness of a cervical airbag in mitigating neck extension and lateral flexion under varying low impact energy and airbag inflation levels. Two finite element environments were developed for neck extension and lateral flexion conditions, utilizing Hybrid-III 50th percentile and Powered-Two-Wheeler finite element dummy models respectively, and were validated referring to experimental data of mentioned systems. The results showed consistent reductions of neck range of motion when an airbag was utilized, decreasing the angles up to 40% without compromising head kinematic responses, tied to traumatic brain injuries; but the scale of this effect was decreasing as impact energies were elevated. Further research must evaluate these relationships in moderate and high energy impact scenarios, possibly also including directional variability.

Keywords Cervical airbag, cyclist safety, injury prevention, virtual testing, vulnerable road users

I. INTRODUCTION

Cyclists remain the only road users that have not had a significant decline in the number of road fatalities in the last decade, as opposed to all other traffic participants, both in the EU and USA [1-2]. Cyclist fatalities globally correspond to 5% of total traffic deaths [3]. Additionally, studies have shown that, with the exception of fatality cases, underreporting of cyclist incidents is a frequent phenomenon all over the world. Only 8% of total injurious cyclist incidents are reported to the official accident database and the majority of the injured receive neither police action, nor medical treatment afterwards the incident [4]. Such numbers align with findings that underreporting of injuries is most likely for cyclists out of all road user groups [5-6]. As the prevalence of cyclist injuries would be much greater accounting for such underreporting, an in-depth overview of the cyclist incident injuries and their mechanisms is needed.

For years, the most severe and often occurring injuries among cyclists have been head-related [9-13]. It is clear that the most effective passive safety equipment currently used by cyclists is the helmet. Helmets have been designed to mitigate translational effects, and more recently rotational ones as well, with broad consensus on helmet effectiveness in reducing head and brain injuries that are associated with the above mentioned kinematics [8][14-16]. Studies on helmet use and head injury relationship have shown reductions of up to 51% in head injuries, 33% in facial injuries, and 65% in fatal head injuries [16]. However, it is true that cyclists are also exposed to high risk of injuries to other body regions. For this study cervical spine injuries (CSIs) will be emphasized.

Injuries of the upper cervical spine generally occur because of significant forces applied to the head during trauma [7]. This relationship alone can spark interest for deeper understanding of such injuries, since most cyclist head injuries are a result of a blunt force impact [13]. A study in Norway showed that the most common injury presenting concomitantly with a CSI was head trauma, identified in 31% of all CSI cases, isolated and with additional injuries present. In fact, the previous study identified cycling as the second most common cause of CSIs. The most common CSIs in cyclists were C6/C7 fractures, occipital condyle fractures (OC-Fx), and C5/C6 fractures. It was stated the mechanism behind the OC-Fx in bicyclists could be a combination of rotation and compression forces in the C0/C1 joint as the cyclist goes over the handlebars and hits the ground headfirst [14]. Other sources have shown an increase of these cyclist injuries over the last years [18-19].

While helmets have been performing outstandingly in mitigating or preventing cyclist head injuries, efforts to show effectiveness of helmet wearing in reducing cyclist CSIs have been less successful, and there is no clear evidence for a reduction in CSIs provided by helmet use [14][16-17][20-21]. To tackle this gap from the mobility safety perspective, some recent helmet designs have begun to integrate airbags, with a primary aim to increase

E. Jokubaityte (e-mail: ejokubaityte@comillas.edu) is an MsC. Eng. and Research Assistant, J. M. Asensio-Gil is a PhD candidate and Research Assistant, and Dr M. Valdano, Dr C. Rodriguez-Morcillo and Dr F. J. Lopez-Valdes are Associate Professors and Researchers at MOBIOS Lab, Institute for Research in Technology (IIT), Comillas Pontifical University in Madrid, Spain. Dr J. A. Carroll is a Senior Research Specialist in Biomechanics at Autoliv. N. Oleaga-Ortega and L. Llobet-Cusi are co-founders of EVIX, located in Mataró, Spain.

protection for the head and possibly the cervical spine [22-24]. Design decisions mainly propose the airbag either positioned around the neck or additionally surrounding the helmet completely upon inflation. Such airbags initially aim to restrict the motion of the head, provide kinetic energy dissipation (as it deflates upon contact with a hard surface) and so, decrease cervical forces and moments [23].

Hövding 2.0 is an airbag helmet designed to improve cyclist protection during impact by deploying an airbag that surrounds the helmet and the neck. Past studies have evaluated the effectiveness of this equipment, measuring reductions in the peak linear and rotational accelerations of the head, and in head injury criterion (HIC) values when compared to other helmets without airbags. In shock absorption tests, the Hövding recorded a peak linear acceleration of 48 g, one third of the average of 175 g measured with other conventional helmets [23-24]. Another study tested a different helmet airbag in two impact velocity load cases, where the airbag did not deploy in the first test of 6.86 m/s impact velocity and was deployed in the second of 11.1 m/s impact velocity. The criteria used for assessing CSI were lower in the test in which the airbag deployed, despite the higher impact velocity. This suggested that helmet airbags can reduce cervical loading in cyclists during impacts [22]. A novel airbag helmet design has been tested in a finite element (FE) environment, comparing its effectiveness in mitigating traumatic brain injuries versus a conventional helmet [25]. Similar findings were presented: the airbag helmet reduced peak forces applied to the head, decreasing peak linear acceleration and delaying its peak, resulting in lower values of Head Injury Criteria (HIC36) maximum principal strain (MPS) of brain tissue.

Despite these studies, there is still insufficient information on the performance of airbag helmets in full-scale tests or on their effectiveness in constraining cervical spine motion, in combination with possible head trauma. A pilot study was designed to preliminarily investigate the relationship [26]. Three different cervical airbag designs were evaluated in neck extension scenarios, where the Hybrid III 50th percentile male anthropometric test device (ATD) was laid supine on and constrained to a rigid horizontal surface which was dropped from 50 cm height, impacting another rigid surface. Three baseline tests were performed with no airbag, followed by two repetitions for each inflation level of every airbag, amounting to 21 tests in total. All tested cervical airbag designs showed effectiveness in reducing the range of cervical extension in cyclists, with the best-performing one resulting in reductions of up to 35%. The results obtained suggested that flexible limitation of head extension does not increase the risk of head injuries but could contribute to a decrease in the risk of cervical injuries. With the study providing validation data for FE simulation-based studies, the best-performing airbag model was then implemented in an FE environment, and after validating the complete system, a parametric study was carried out by varying the airbag pressure and impact energy levels [27]. A more recent study explored the effectiveness of this airbag design in reducing neck lateral flexion by performing 16 experimental tests with the Powered-Two-Wheeler ATD laid laterally on and constrained to a rigid horizontal surface, which was dropped from 10 and 20 cm and impacted a damped surface [28].

The parametric study to be presented here is a continuation of work presented in [27] in a sense that the varied parameter matrix is updated, a more detailed cervical airbag FE model is introduced, as well as intent to improve overall FE environment boundary conditions to acquire more precise model predictions. Additionally, this study introduces the implementation and parametrization in FE environment of lateral flexion scenarios.

The aim is to perform a parametric study of varied airbag pressure and impact energy values, with the objective to deepen the understanding of the relationship between cervical airbag use, its ability to reduce neck range of motion (ROM) and the assessment of the influence of these changes in ATD head injury metrics in extension and lateral flexion scenarios by comparing kinematics and dynamics of the systems.

II. METHODS

Two finite element (FE) systems were developed, recreating the experimental setup boundary conditions, for cervical extension condition as recorded in [26], and for the cervical lateral bending condition as published in [28]. Both experimental test rig setups are presented in Fig. A1. The data used for validation was derived from test setups with the Hybrid III 50th percentile male anthropometric test device (ATD) in vertical falls of 0.5 m in a series of 9 physical tests for the neck extension condition, and of Powered-Two-Wheeler ATD vertical falls of 0.1 m and 0.2 m in a series of 16 physical tests for the neck lateral flexion condition. The ATD models in the FE experimental testing environment were positioned utilizing the combination of photo images from experiments, the measurements of key landmarks and 3D scans of initial position. Definitions of boundary conditions in FE were validated by comparing the FE ATD response against the experimental testing data. Means of validation were

kinematic response comparison and an objective rating metric based on the ISO/TS 18571 [29] for evaluating correlation between experimental and simulation signal responses. The simulations were carried out using LS-DYNA MPP R9.3.1 (ANSYS/LST) software, pre-processing using PRIMER (Oasys Ltd.), post-processing D3PLOT (Oasys Ltd.) and META (Beta CAE Systems).

Generic Cyclist Helmets and Cervical Airbag FE Model Development

The helmet and the cervical airbag prototype (EVIX S.L.) FE models were created from 3D scans of the equipment used in the experimental testing. The primary scan files were processed with focus on acquiring final and geometries of the models. The meshing was performed in ANSA (Beta CAE Systems), following the general mesh quality criteria of skewness, aspect ratio and orthogonality, while balancing node count optimization for computational time. As the physical airbag prototype was manufactured from typical automotive-application airbag material, the airbag model material is fabric-type, with its properties taken from a generic airbag FE vehicle model [30]. In the experiments, the purpose of the helmet was to serve as a boundary condition for the airbag position and motion during the impact. This raised the importance of obtaining exact helmet geometries, but eliminated the need for unique material definitions as the helmet did not receive any impact during the experiments. Therefore, the helmet material definition was simplified to be rigid; parallel to what was done in the experimental setups, two helmet FE models of distinct geometries were developed for each impact case environment, both corresponding to their physical weight (by introducing correspondent density values).

Neck Extension FE Environment Setup for Validation

The main elements of the environment for neck extension consisted of the Hybrid III 50th percentile male (H3) FE model (ATD-MODELS GmbH), the rigid table on which the ATD is positioned, the rigid cargo strap geometry entities for ATD constraint, a generic cyclist helmet and a prototype cervical airbag.

The H3 FE model was positioned to match the initial posture from the experimental testing based on photo images, as displayed in Figure 1, and measurements taken before the tests. The H3 was constrained to the table using heavy-duty cargo straps that did not provide absolute constraint of thorax movement during impact, which led to contributions to overall neck extension. It was concluded that in the FE environment the ATD thorax must also retain a controlled degree-of-freedom (DOF) in Y-axis rotation. This was implemented by creating strap parts in FE and compressing the ATD in a way that provides accurate thorax DOF control. Straps were positioned by superposition, as seen in Figure 2.

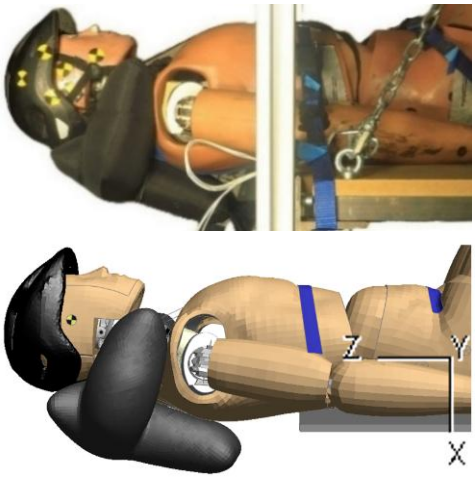

Fig. 1. H3 initial position in experimental testing (top) and in FE environment (bottom)

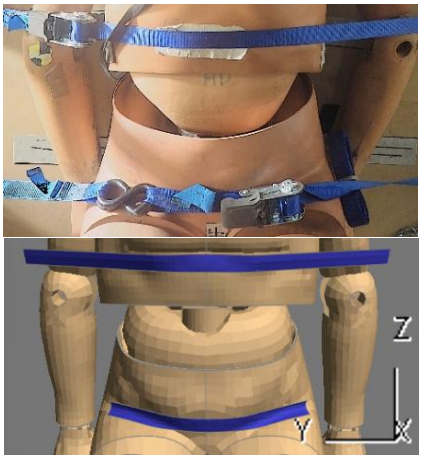

Fig. 2. Restraining heavy-duty cargo strap position for torso and pelvis in experimental testing (top) and in FE environment (bottom)

To create an optimal torso and pelvis compression preceding the impact phase, a specific translational displacement was applied to the straps beforehand, with the aim of maintaining correct elastic dummy deformation. The simulation termination time was 450 ms, with key intervals of 0–100 ms, meant for ATD compression, 100–250 ms for ATD settling, and 250–450 ms for the impact phase.

The neck extension was observed in a rear impact scenario. The load case is realized as an inverted acceleration

curve that is applied to the rigid table. The curve was characterized by experimental testing measurements, acquiring an average acceleration pulse of the 9 physical tests, from the impacting table accelerometer data.

Neck Lateral Flexion FE Environment Setup for Validation

The main elements of the environment for neck lateral flexion consisted of the Powered-Two-Wheeler (PTW) Dummy [31] FE model (Humanetics), rigid table on which the ATD is positioned, a generic cyclist helmet and a prototype cervical airbag.

To match the weight and biofidelity of the ATD behavior during testing, the arms and the legs above knee were removed for the PTW FE model. Then it was positioned using a 3D scan of the initial position from the experiments (Figure 3).

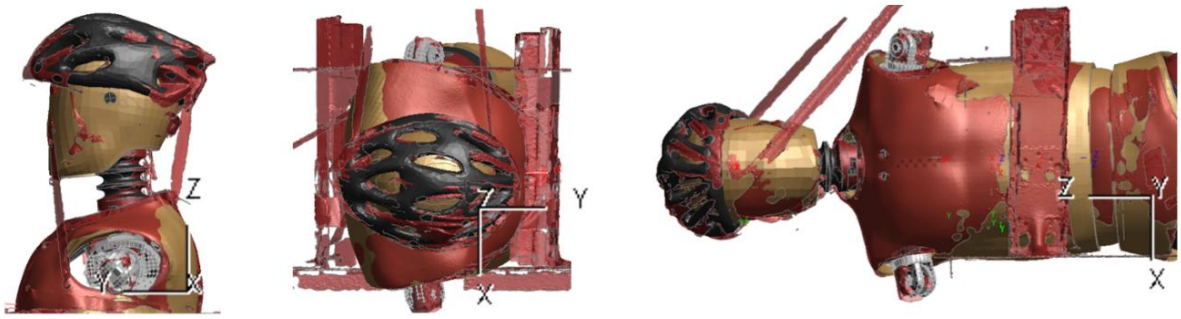

Fig. 3. PTW FE model positioned against 3D scan of the ATD in experimental initial position

The boundary conditions in this experimental testing ensure complete constraints upon the ATD body below the neck and there were no, or negligible, contributions of thorax rotation to the overall neck flexion during impact. This allowed implementation of rigid body constraints upon the PTW FE model body below the neck.

Two lateral impact load cases were acquired for the neck lateral flexion, corresponding to 0.1 m and 0.2 m falls. There were 16 experimental samples for each fall height, and the acceleration curves used as input in the FE models were acquired as the average of the 16 measurements. Given that the experiments were carried out with low energy impacts which were also damped in this lateral case (unlike the undamped neck extension tests), after trial and error it was determined that for this FE environment it is crucial to simulate the fall phase for it to provide a response with reasonable correlation to the experimental data. Simulation termination time that allowed the observation of maximum flexion for both fall heights was 400 ms.

Cervical Airbag Positioning and Boundary Conditions

The cervical airbag prototype had no ventilation hole and had constant pressure supply throughout the experimental testing. For this reason, in FE LS-DYNA environment, the airbag was defined using *AIRBAG_SIMPLE_PRESSURE card, inputting a desired initial pressure value, which later corresponded to the changes of airbag volume during impacts. For both neck extension and lateral flexion scenarios, the cervical airbag was positioned using photo images from experimental testing, as seen in Figure 4 (where an image of the model is overlaid onto an image from the physical experiment).

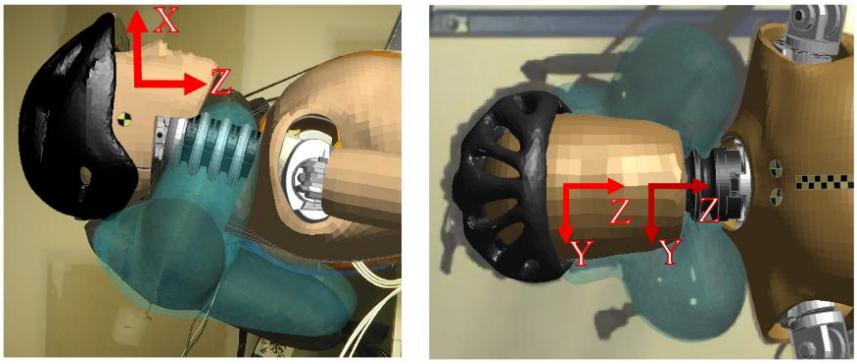

Fig. 4. Cervical airbag position against experimental photos for neck extension (left) and lateral flexion (right)

In both scenarios, the airbag positioning procedure was the same. The desired pre-impact position required separate positioning pre-simulations, where the airbag is first offset from the ATD surface and has 3-4 permanently pretensioned springs attached to the ATD pulling it into place, a method commonly used in simulation to reach the desired initial position. The airbag would be inflated minimally (0.03 bar) to keep geometrical integrity and still allow it to be pushed to the front of the neck. In the beginning of impact simulations, the positioned airbag would be dynamically inflated from 0 bar to the desired pressure level; it was confirmed that it had no effect on the initial positions of ATD head and neck.

Conditions to fix the airbag to the ATDs were implemented in the FE environments with great attention to the airbag kinematic behavior and physical realization differences found in neck extension and lateral flexion cases. The solutions in FE utilized stiff springs connecting the airbag front arms to the chest of the H3, and to the chin for the PTW. Additionally, with the H3 there was another stiff spring connecting lower part of the airbag with upper back of the H3, while the PTW had a few constrained nodes at the top of the airbag to the back of the helmet. Stills of simulation and experiment, highlighting airbag kinematic behaviors can be referred to in Fig. A2.

Validation of the FE Environments

In total there were 12 different cases of experimental testing available for FE simulations validation, 4 for neck extension and 8 for neck lateral flexion scenarios. The detailed characterization matrix for the cases can be seen in Table I.

TABLE I

PARAMETRISATION MATRIX FOR FE ENVIRONMENT VALIDATION

Neck Extension			*Neck Lateral Flexion*					
Test no.	Airbag Pressure, bar	Fall height, m	Test no.	Airbag Pressure, bar	Fall height, m	Test no.	Airbag Pressure, bar	Fall height, m
H3_01	0 (no airbag)	0.5	PTW_01	0 (no airbag)	0.1	PTW_05	0 (no airbag)	0.2
H3_02	0.1		PTW_02	0.1		PTW_06	0.1	
H3_03	0.15		PTW_03	0.15		PTW_07	0.15	
H3_04	0.2		PTW_04	0.2		PTW_08	0.2	

Firstly, a kinematic comparison was carried out, putting simulation result animations on top of corresponding experimental video, then individual responses of signals were compared. Such signals for neck extension cases were head center of gravity (CoG) resultant acceleration, angular velocity in Y and neck extension angle. For neck lateral flexion cases they were head CoG accelerations in Y and Z, angular velocity in X and neck flexion angle, and additionally upper neck force in Y (shear) and moment in X (bending). All mentioned axes are corresponding to the ATD's local coordinate system of the signal related sensor and can be consulted in Figure 4. Neck range of motion in both extension and lateral flexion is expressed by integrating the signals of head angular velocity in the respective axis for the load case. Afterwards, a correlation analysis was carried out based on ISO/TS 18571 standard, with the parameters used for calculation left as standard-defined defaults. Since the metric allows 1 reference curve per correlation score, an average is acquired after separate correlation analyses are made for all existing signal references. All experimental testing scenarios had 2 repetitions per configuration, with the exception of "no airbag" scenario for neck extension cases having 3 repetitions.

Parametric Study Characterization

TABLE II

PARAMETRIC STUDY VARIABLES MATRIX

Neck Extension				*Neck Lateral Flexion*				
Height, m / Pressure, bar	0.5	0.75	1.0	Height, m / Pressure, bar	0.2	0.3	0.4	0.5
0 (no airbag)	H3-.5_0	H3-.75_0	H3-1_0	0 (no airbag)	PTW-.2_0	PTW-.3_0	PTW-.4_0	PTW-.5_0
0.1	H3-.5_.1	H3-.75_.1	H3-1_.1	0.1	PTW-.2_.1	PTW-.3_.1	PTW-.4_.1	PTW-.5_.1
0.2	H3-.5_.2	H3-.75_.2	H3-1_.2	0.2	PTW-.2_.2	PTW-.3_.2	PTW-.4_.2	PTW-.5_.2
0.3	H3-.5_.3	H3-.75_.3	H3-1_.3	0.3	PTW-.2_.3	PTW-.3_.3	PTW-.4_.3	PTW-.5_.3
0.4	H3-.5_.4	H3-.75_.4	H3-1_.4	0.4	PTW-.2_.4	PTW-.3_.4	PTW-.4_.4	PTW-.5_.4
0.5	H3-.5_.5	H3-.75_.5	H3-1_.5	0.5	PTW-.2_.5	PTW-.3_.5	PTW-.4_.5	PTW-.5_.5

The two varied parameters in this study are impact energy (controlled through the fall height) and airbag pressure, and the complete parametric study matrix can be consulted in Table II. A total of 42 simulations were completed, 18 for rear impact and 24 for lateral impact configurations. The ATDs response signals analyzed in the parametric study were the ones used for system validation.

Airbag pressure parametrization is straightforward in LS-DYNA; however, impact energy variation required a separate scaling procedure. Firstly, the theoretical velocity value right before the impact (maximum) for each falling height of interest was calculated from potential and kinetic energy equation tradeoff:

$$\frac{1}{2}mv^2 = mgh \quad \Rightarrow \quad v = \sqrt{2gh}\,, \tag{1}$$

where m is mass (kg), v is velocity (m/s), g is constant acceleration due to gravity (m/s^2) and h is fall length (m).

Then impact acceleration pulse scaling factors for defined impact height variations were calculated in the following manner:

$$SF_i = \frac{v_i}{v_1}, \tag{2}$$

where SF_i is the case scaling factor, v_i is case maximum velocity and v_1 is the initial (reference) maximum velocity.

Injury Assessment

For each virtual test, injury criteria (IC) metrics of brain maximum principal strain (MPS) prediction using DAMAGE metric, and brain injury criterion (BrIC, MPS-based) were calculated, utilizing equations 3 and 4 [32-33].

$$BrIC = \sqrt{\left(\frac{\omega_x}{\omega_{xC}}\right)^2 + \left(\frac{\omega_y}{\omega_{yC}}\right)^2 + \left(\frac{\omega_z}{\omega_{zC}}\right)^2}\,, \tag{3}$$

$$DAMAGE = \beta max_t\{|\vec{\delta}(t)|\}\,, \tag{4}$$

Probabilities for mild traumatic brain injury (TBI) were derived from the associated abbreviated injury scale (AIS2) curves by using established risk relationships for the assessed IC metric values [32].

As for the assessment of cervical injuries, reductions in neck ROM, and, where applicable, neck forces and moments were considered as proxy variables to characterize the risk of cervical injury.

III. RESULTS

Validation of the FE environments

The individual signal correlation analysis scores for each configuration from validation matrix (Table I) can be consulted below in Table III for H3 and Table IV for PTW validation cases.

TABLE III

ISO/TS 18571 CORRELATION SCORE R FOR NECK EXTENSION CASES

		H3_01	H3_02	H3_03	H3_04
Head	Resultant Acc.	0.632	0.650	0.657	0.655
	Angular Vel. in Y	0.751	0.796	0.776	0.761
Neck	Extension Angle in Y	0.701	0.854	0.858	0.851

TABLE IV

ISO/TS 18571 CORRELATION SCORE R FOR NECK LATERAL FLEXION CASES

		PTW_01	PTW_02	PTW_03	PTW_04	PTW_05	PTW_06	PTW_07	PTW_08
Head	Acc. in Y	0.605	0.531	0.473	0.421	0.674	0.591	0.539	0.609
	Acc. in Z	0.665	0.656	0.588	0.432	0.735	0.663	0.621	0.629
	Angular Vel. in X	0.751	0.773	0.621	0.451	0.770	0.714	0.670	0.681
Upper Neck	Flex. Angle in Y	0.752	0.879	0.774	0.631	0.822	0.820	0.779	0.780
	FY	0.726	0.837	0.825	0.726	0.865	0.811	0.833	0.831
	MX	0.751	0.665	0.540	0.561	0.797	0.659	0.590	0.673

Scores of R > 0.94 correspond to “Excellent”, 0.8 < R ≤ 0.94 to “Good”, 0.58 < R ≤ 0.8 to “Fair” and R ≤ 0.58 to “Poor” correlation analysis results. Figures A3 – A7 can be referred to for a more detailed comparison of specific ATD signal agreements between experiment and simulation. In general, the models were able to capture the time behavior and the changes in magnitude of the parameters studied for the different load cases, despite slight differences in peak values.

Parametric Study with The Computational Model

Below, figures 5 and 6 show the analyzed simulation signal responses in minimum and maximum fall heights, for neck extension and lateral flexion conditions. In each graph, six simulation responses with varied airbag pressure in the same energy impact are plotted. The complete versions of the figures with all signal and impact energy responses can be found in the annex, also supplemented by additional tables with the absolute maximum peak value for each signal. The neck extension simulation responses are plotted from t = 250 ms, which corresponds to the beginning of the impact scenario (i.e. after allowing time for pre-impact settling).

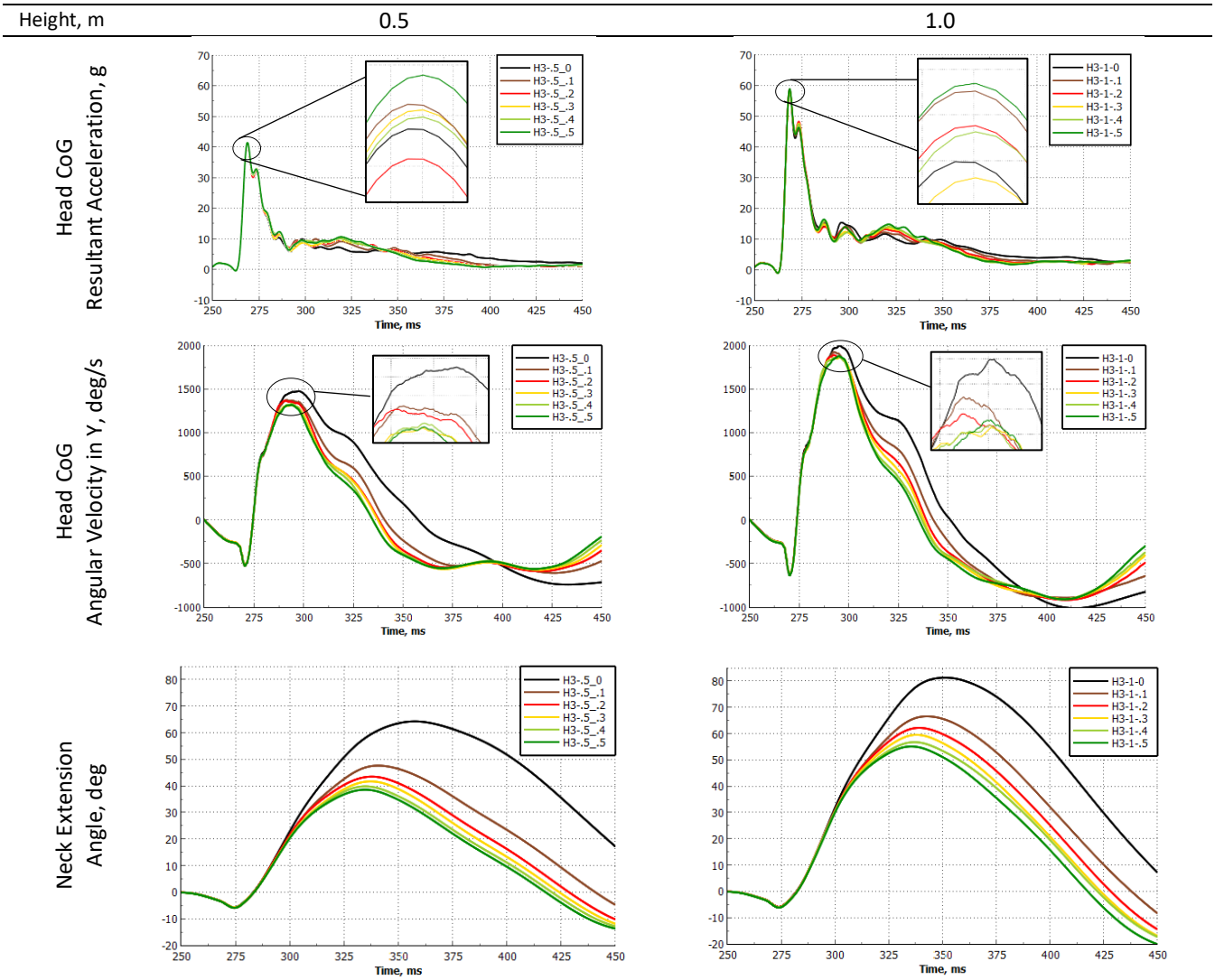

Fig 5. Simulation responses for min (left) and max (right) height neck extension case configurations

In these neck extension scenarios, the responses for head resultant acceleration throughout all heights and airbag pressures vary only a little. For head angular velocity and neck extension angles, maximum value peaks are reached in cases when no airbag was utilized, and the peaks decrease with larger airbag inflation values. With increasing airbag pressures, the duration of neck extension is decreasing, and the peak value is reached earlier.

The peaks of the head resultant acceleration were reached right after the systems were subjected to the maximum impact acceleration, which is at 265 ms. As the head and neck of the ATD were released from all motion constraints starting from 250 ms, negative head angular velocity and longitudinal flexion were observed due to the applied constant gravity load.

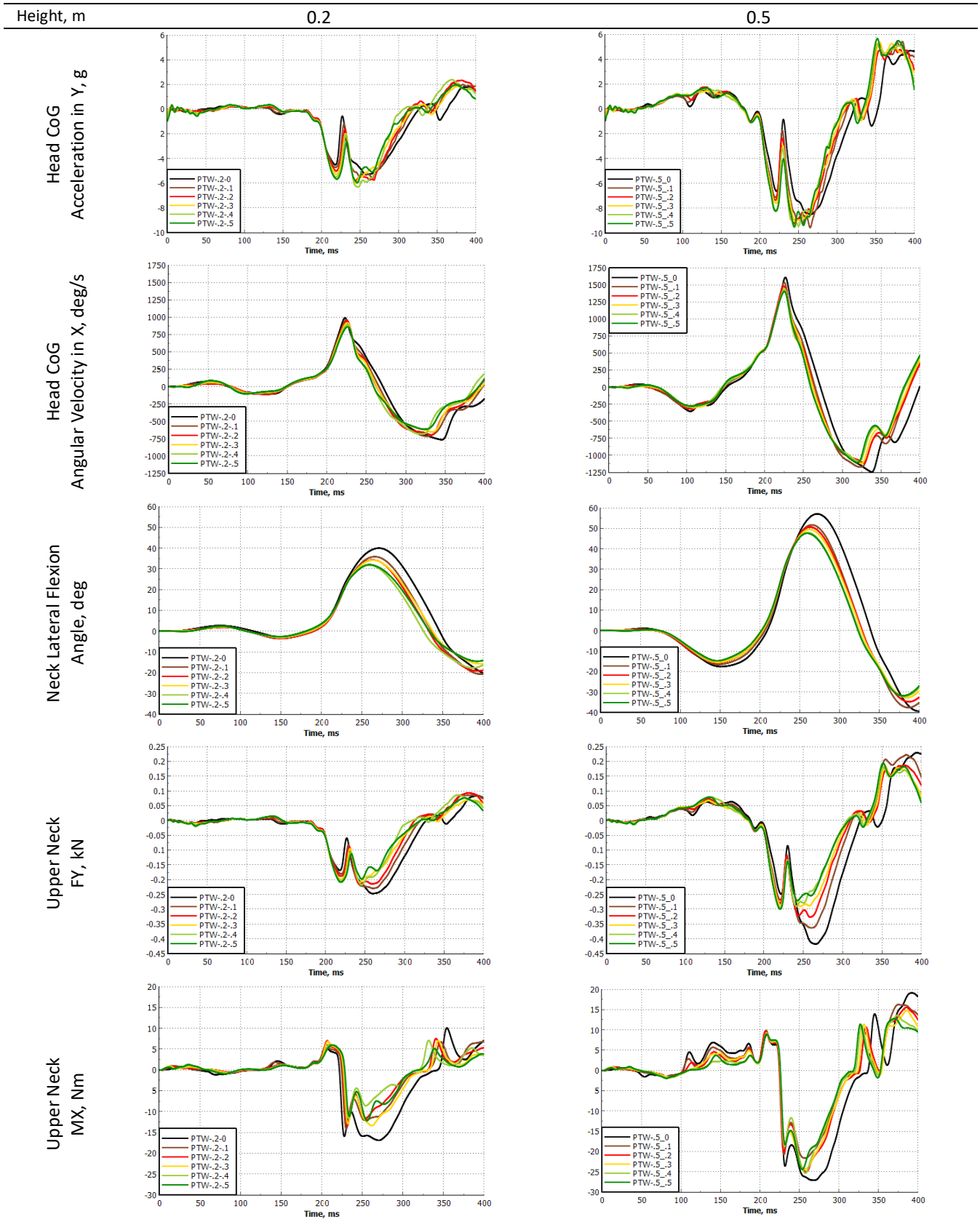

Fig 6. Simulation responses for min (left) and max (right) height neck lateral flexion case configurations

For neck lateral flexion cases, head acceleration peak values were the lowest when no airbag was used, with small increases when one was applied, showing no consistent trends with airbag pressure. Head angular velocity and neck lateral flexion angle results throughout these configurations showed the same patterns as observed for H3 in associated responses, where peak values were reached for cases with no airbag. The peak values and flexion durations were reduced as airbag inflation was increased. Upper neck shear force results were of the same

pattern as the neck flexion angles and head angular velocities. Upper neck bending moment reached peak values across heights when no airbag was used, and maximum peak moment values were reduced with introduction of the airbag. Minimum peak values of the bending were inconsistent throughout airbag inflation pressures.

Figure 7 represents all simulation configurations with the airbag responses relative to the baseline (no airbag) cases, comparing the extension and flexion angles for rear and lateral impact scenarios. Figure 8 has the same relative-value comparison carried out for lateral impact upper neck responses of force in Y-axis and moment about the X-axis.

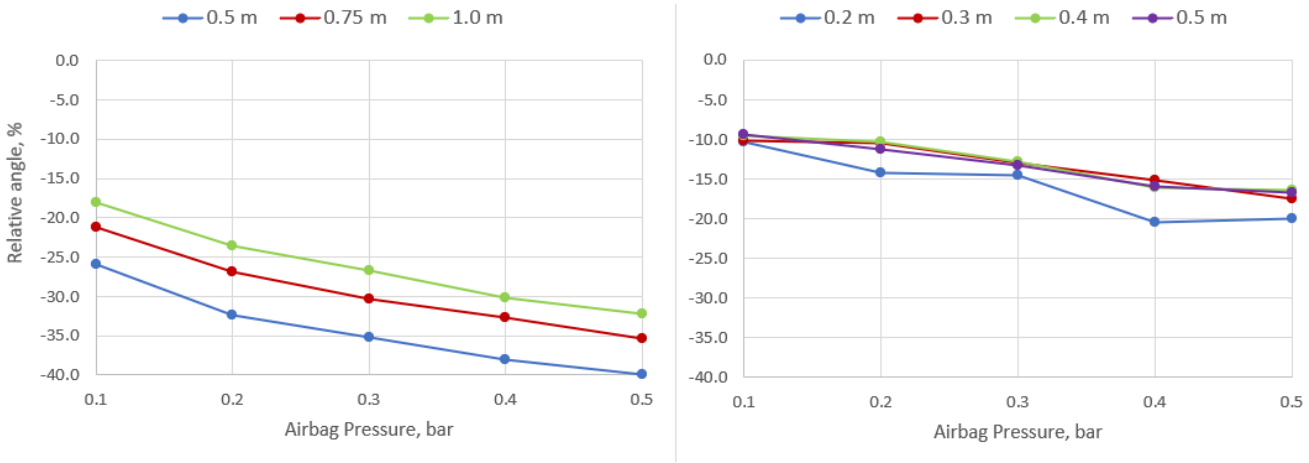

Fig. 7. H3 extension (left) and PTW lateral flexion (right) angle values, relative to the “no airbag” scenarios in all impact heights

The neck range of motion (ROM) in both H3 and PTW, in respect to the baseline cases was always decreased when an airbag was utilized. The angles were reduced more as the airbag pressure was increased, with a linear pattern shown regardless of drop height setting. The extension neck angle experimented relatively lower reductions with airbag of any pressure used when dropping height was increased. The relative decrease in lateral flexion was not dependent on impact heights within the range studied.

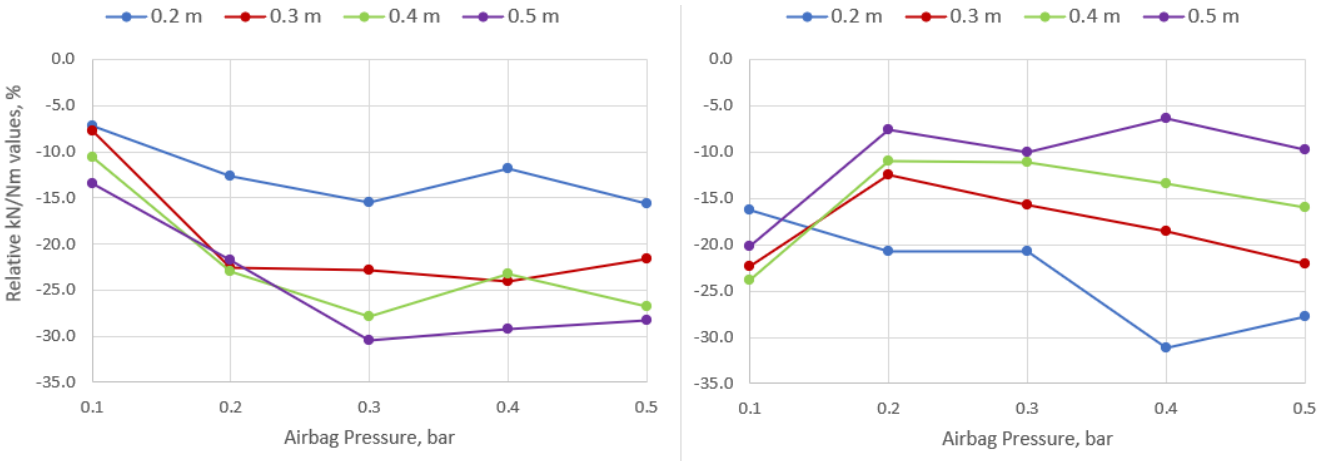

Fig. 8. PTW upper neck FY kN (left) and MX Nm (right) values, relative to the “no airbag” scenarios in all impact heights

PTW upper neck response peak values of shear force and bending moment were always smaller when an airbag was utilized compared to the baseline cases. With airbag inflation of 0.1 bar, both signal responses had the least difference throughout heights (<10%). Larger dispersions were introduced as the pressure level was increased. Height had the opposite effect on the responses; where FY was reduced relatively the most in the maximum, and MX in the minimum height settings. The relative shear force decrease grew from 0.1 to 0.3 bar, then showed similar effects at 0.3 to 0.5 bar inflation pressures throughout fall height settings. With larger airbag pressures, the bending moment decreased inconsistently in the lowest impact setting. but increased in the highest fall setting.

Brain Injury Prediction

AIS2 injury probability predictions by BrIC and MPS-DAMAGE metrics are presented in Table V, for both rear and lateral impact cases.

TABLE V
AIS2 INJURY PROBABILITY (%) PREDICTION BY MPS-DAMAGE / BRIC FOR REAR (LEFT) AND LATERAL (RIGHT) IMPACT CONFIGURATIONS

Height, m / Pressure, bar	0.5	0.75	1.0	0.1	0.3	0.4	0.5
0 (no airbag)	14.4 / 40.5	20.9 / 57.2	24.9 / 70.5	0.4 / 14.2	0.9 / 25.1	1.2 / 34.6	1.5 / 43.4
0.1	14.3 / 34.6	19.3 / 48.8	25.7 / 66.7	0.5 / 13.1	0.7 / 22.0	1.0 / 30.6	1.2 / 39.4
0.2	15.0 / 34.1	19.1 / 48.7	26.0 / 64.9	0.7 / 12.7	0.8 / 21.1	0.9 / 29.4	1.5 / 37.9
0.3	13.6 / 31.2	18.7 / 47.9	26.3 / 63.4	0.8 / 12.0	0.9 / 20.1	1.1 / 28.8	1.5 / 36.6
0.4	13.7 / 31.9	18.7 / 48.2	26.8 / 63.7	0.9 / 11.1	0.9 / 19.5	1.5 / 27.5	2.0 / 36.3
0.5	13.4 / 31.5	18.5 / 48.4	24.7 / 64.3	0.7 / 10.3	1.0 / 18.9	1.3 / 27.5	1.6 / 35.0

The MPS-DAMAGE metric predicted 13.4 - 26.8% probabilities of AIS2 injury in rear impacts, and 2% or smaller probability of sustaining one in tested lateral impacts. It also predicted probabilities of less difference between pressures in the same height configuration than the BrIC metric; the latter injury criteria consistently showed the largest probability of AIS2 injury when the cervical airbag was not utilized, as opposed to DAMAGE-based predictions showing no such pattern.

IV. DISCUSSION

As there is no clear evidence of helmet effectiveness in cervical spine injury (CSI) mitigation, new implementations of head and neck protection for cyclists have been raising interest. Studies have looked for clues of a positive performance of cervical airbags for cyclists, mainly showing promising results, and thus enabling further analysis of various equipment solutions [22-23][26]. In this parametric study, it was chosen to observe the influence of low impact energies and cervical airbag pressures to airbag effectiveness in reducing neck range of motion, which is assumed to decrease the risk of sustaining CSI. Neck flexion and extension magnitudes can be associated to possible cyclist CSIs; as exceeding the natural range of motion of the cervical spine is shown to end up in cervical spinal segment failures [34]. It is also important to acknowledge that possible trade-offs between predicted injury severities have been observed, particularly an increase in brain injury possibility when reduction of neck extension angles is prevalent [27]. The main goal in the current study was to analyze the effectiveness of the cervical airbag in neck ROM reductions with different airbag inflation pressures and how it affects the rotational velocity of the head and metrics related to head injury risks.

In rear impact scenarios, it can be seen that airbag presence has little contribution to the peak values of head resultant acceleration. In case of lateral impacts, which were of even lesser severity, it was observed that an airbag of any inflation slightly increases the head accelerations. However, in none of the 42 cases it was of significant value that would suggest an actual increased risk of head trauma. It is considered here that in these low energy impacts, cervical airbag inflation pressure or equipment's presence altogether does not influence significantly the acceleration of the dummy head.

Head angular velocity peak values in both impact cases were decreased with any inflation level of an airbag, comparing to "no airbag" cases. The most effective reductions of up to 11%, in all heights for H3 were noticed with a 0.3 bar airbag, although comparing to 0.4 and 0.5 bar configurations, the difference is <1%. For PTW, the angular velocity peaks were reduced up to 13.5%, and the airbag pressure, which showed the largest reductions throughout heights, was 0.5 bar. It could be suggested that higher pressure airbags (0.3-0.5 bar) are more efficient in reducing angular velocity peaks when the user is subjected to low-energy rear or lateral impacts. When looking into the neck extension and flexion angles, airbags of whichever inflation successfully decreased the ROM angle by 9.4 to 19.9% for lateral, and from 18.1 to 40.0% for rear impacts, and the specific inflation pressure of 0.5 bar offers the largest percentage decrease in both scenarios. A clear trend of "larger inflation pressure – larger relative neck extension/flexion reduction" can be observed in all analyzed impact cases (Fig. 5). However, it is also observed that the airbag effectiveness of decreasing the ROM of the neck is at its best when subjected to the lowest energy impacts, suggesting that further exploration of such response when the VRU is subjected to

moderate or high impact energies would be useful.

Additionally, for PTW there was a possibility to validate upper neck response signals and thus include them in the analysis of the parametric study. It can be observed that the use of the airbag successfully decreases upper neck shear force (FY) and bending moment (MX), with force most reduced up to 30.4% and moment up to 31.1% relative to the no airbag cases. It is noted that the shear force is decreased most effectively in higher impact energies, while the bending moment mainly shows the opposite. FY was lowest with higher airbag pressures (0.3-0.5 bar), while MX response trends were not as conclusive when comparing inflation pressures. However, a worthy observation is of the relative FY and MX reductions being the least variable (<10%) throughout different height settings when an airbag of 0.1 bar inflation was utilized, when other inflations showed large differences in reduction effectiveness throughout impact heights. This could suggest that an airbag with lower pressure level may offer more controlled upper neck responses throughout differed impact energy scenarios; however, possibly with a compromise of effectiveness levels in other important head and neck kinematic response reductions.

AIS2 Traumatic brain injury probability prediction showed large differences based on used calculation metric, with MPS-DAMAGE predicting 13.4 – 26.8% for H3 and <2% for PTW, while calculated using BrIC mild TBI probability was 31.2 – 70.5 % for H3 and 10.3 – 43.4 % for PTW. The BrIC metric suggested lowest probability of AIS2 brain injury in cases where an airbag was worn with higher inflation rates (0.3 – 0.5 bar) for both extension and flexion cases. There are no patterns to be noted for injury prediction using MPS-DAMAGE, where the probability seems to be independent of the airbag inflation rate.

Overall, the findings presented here suggest that in low-energy impacts, use of an airbag of any inflation is able to reduce neck extension and lateral flexion angles without increasing the predicted traumatic brain injury risk. While this performance is less effective in lateral impacts, the airbag decreases shear force and bending moment in the upper neck, which are associated with cervical spinal segment failure. A conclusion could be drawn that relatively higher airbag pressure levels of 0.3 – 0.5 bar offer maximized kinematic, dynamic response and TBI probability reduction effects in low-energy impacts. However, for most kinematic responses, the mentioned airbag performance effectiveness gradually declines as impact energy is elevated, suggesting that different trends may be observed in moderate or high impact scenarios.

The first limitation that must be assessed in this study is the performed validation of FE models and how reliable it makes the previously discussed results. While all R scores for rear impact scenarios are “Fair” or “Good”, disagreement can be observed for lateral impacts, from PTW_01 to PTW_04 cases and for one signal from PTW_07 case. The main hypothesis for the lower correlation scores would be the low energy load case that the ATD is subjected to in both experimental and virtual testing (maximum peaks of 6.6 and 8.4 g, for 10 and 20 cm falls respectively). As the utilized crash dummy is equipped with high-measuring-range accelerometer (500 g), it is possible that there could be larger errors introduced between the acquired experimental and virtual testing measurements. Additionally, as overall absolute values of the response signals are less extreme, corridors created during correlation analysis are smaller and will penalize the correlation score more than it would, compared to signals of large absolute value distribution. For the lateral impact 20 cm fall cases, it was noted that all of response signals showed “Fair” or “Good” except for one case with a “Poor” correlation for one of the head acceleration components, even if the impact pulse was increased only slightly. This change in correlation scores suggested that the FE model is more accurate when subjected to higher energy loading, and that the parametric study could provide useful data. In-depth observations could be made for neck range of motion and upper neck loading as these signals showed the highest correlation, while readings of translational head acceleration should be treated cautiously.

It is also important to understand the motivation and credibility of this parametric study variable matrix. The variable of airbag inflation level was introduced because the validation models were able to predict the ATD response's distribution pattern when comparing them between all airbag pressures. The reason for the introduced fall height variation was to provide insight into possible trend changes in the ATD responses of interest. Further studies are needed to analyze the performance of this airbag prototype or of a similar design in different environments; the study presented here could aid in defining the main boundary conditions or specific test matrix of variables, if the observed model predictions of interest are to be confirmed.

Another limitation of this study, applicable to neck extension angle analysis cases, would be the use of Hybrid III 50th percentile male dummy, which is initially validated and mainly used for frontal crashes. This implication might show difference in obtained results, should the same tests, experimental or virtual, be repeated with

human donors, ATDs showing more biofidelity in rear impact cases, or respectively with human body models (HBMs) or the FE versions of said dummies. However, any of the mentioned variations would be encouraged, as another step would be taken towards understanding the full benefits and compromises this cervical airbag design solution could offer to cyclists. The Powered-Two-Wheeler dummy on the other hand, is equipped with WorldSID ATD head and neck – parts of a dummy that is the typical choice in the industry and research, concerning mobility safety, in lateral loading scenarios. A general biofidelity-related limitation, concerning both ATDs used in experimental testing would be the increased stiffness of the neck when comparing it to a human one, for the sake of robustness and reusability of the ATD. Thus, it should be acknowledged that larger neck ROM would be expected in testing that would implement increased biofidelity of the subject.

To add, the FE environments presented in this parametric study were developed to virtually test only low energy impacts. As both experimental testing cases were carried out in lower energy impacts, the boundary conditions that were implemented there may not have been suitable to support increased heights. If the FE environments were refined to provide likely accurate boundary conditions for increased energy impacts, the quality of currently performed validation would have been compromised. This opens an opportunity for future work in testing, both experimental and virtual, for the cervical airbag effectiveness in reducing neck ROM and probability of TBI which could and should be studied further and applied to real-life crash load cases.

V. CONCLUSION

Two finite element systems for observing neck extension and lateral flexion of crash dummies that were subjected to low energy impacts were developed; a validation against associated experimental testing data was performed. A parametric study of virtual testing was carried out with a total of 42 simulations, where no airbag and 5 different airbag pressures were implemented in different fall heights, 3 for extension and 4 height configurations for flexion analysis cases. The use of a cervical airbag in conjunction with a helmet was associated with reductions of both neck range of motion and risk of sustaining a mild traumatic brain injury. Airbag settings with higher levels of inflation pressure were observed to perform as well or better in mentioned reductions than the relatively less inflated options in these tested low energy impact scenarios. However, based on dummy force and moment measurements, an airbag with lower pressure level may offer more controlled upper neck responses throughout different impact energy scenarios. Further studies may continue assessing these relationships when higher energy impacts are implemented with their directional variability, conditions that would be more applicable to challenging equipment needs and, ultimately, end user safety.

VI. ACKNOWLEDGEMENTS

This research was funded by Fundación MAPFRE through the program “Ayudas a la Investigación Ignacio Hernando de Larramendi 2023”. Autoliv and EVIX S.L. made possible the experimental testing by providing access to the crash test dummies and to the airbag prototype, respectively. We would like to thank also the support of Humanetics and ATD Models for providing access to the PTW and Hybrid III models. The content of this manuscript reflects the views of the authors only and does not represent necessarily the position of their associated institutions.

VII. REFERENCES

[1] European Commission (2024) *Road safety thematic report – Cyclists*, European Road Safety Observatory, Brussels, European Commission, Directorate General for Transport.

[2] Kirley, B. B., Robison, K. L. *et al.* (2023) National Highway Traffic Safety Administration, *Countermeasures that work: A highway safety countermeasure guide for State Highway Safety Offices, 11th edition, 2023* (Report No. DOT HS 813 490).

[3] World Health Organization (2023) *Global status report on road safety 2023* [Online]. Available: http://www.who.int/iris/handle/10665/375016

[4] Pauer, G., Krizsik, N., Szigeti, S. (2023) Estimating the Underreporting Rate of Injured Cyclists. Periodica Polytechnica Civil Engineering, Vol. 67(2), pp.619–627.

[5] Watson, A., Watson, B., Vallmuur, K. (2015) Estimating under-reporting of road crash injuries to police using multiple linked data collections. Accident Analysis & Prevention, Vol. 83, pp.18–25.
[6] Elvik, R., Mysen, A. (1999) Incomplete Accident Reporting: Meta-Analysis of Studies Made in 13 Countries. Transportation Research Record, Vol. 1665(1), pp.133–140.
[7] Jackson, S. R., Banit, D. M., Rhyne III, A. L., Darden, B. V. (2002) Upper cervical spine injuries. JAAOS-Journal of the American Academy of Orthopaedic Surgeons, Vol. 10(4), pp.271–280.
[8] Arshad, Z., Majeed, M. *et al.* (2022) Cycling-related trauma admissions to the major trauma centre in the cycling capital of the United Kingdom. Injury, Vol. 53(12) pp.3970–3977.
[9] Eilert-Petersson, E., Schelp, L. (1997) An epidemiological study of bicycle-related injuries. Accident Analysis & Prevention, Vol. 29(3), pp.363–372.
[10] Perrin, A. E. (2012) Cycling-related injury. Connecticut medicine, Vol. 76(8), pp.461–466.
[11] de Guerre, L.E.V.M., Sadiqi, S., Leenen, L.P.H., Oner, C. F. (2020) Injuries related to bicycle accidents: an epidemiological study in The Netherlands. European Journal of Trauma and Emergency Surgery, Vol. 46, pp.413–418
[12] McDermott, F. T, Klug, G. L. (1985) Head injury predominance: pedal-cyclists vs motor-cyclists. The Medical journal of Australia, Vol. 143(6), pp.232–234.
[13] Depreitere, B., Van Lierde, C. *et al*. (2004) Bicycle-related head injury: a study of 86 cases. Accident Analysis & Prevention, Vol.36(4), pp.561–567.
[14] Eng, S. F., Næss, I. *et al.* (2022) Bicycle-related cervical spine injuries. North American Spine Society Journal, Vol. 10, pp.100–119
[15] R. Elvik (2011) Publication bias and time-trend bias in meta-analysis of bicycle helmet efficacy: A re-analysis of Attewell, Glase and McFadden, 2001. Accident Analysis & Prevention, Vol. 43(3), pp.1245–1251
[16] Olivier, J., Creighton, P. (2017) Bicycle injuries and helmet use: a systematic review and meta-analysis. International Journal of Epidemiology, Vol. 46(1), pp.278–292.
[17] Rivara, F. P, Thompson, D. C, Thompson, R. S (1997) Epidemiology of bicycle injuries and risk factors for serious injury. Injury Prevention, Vol. 3(2), pp.110–114.
[18] Broe, M. P., Kelly, J. C., Groarke, P. J., Synnott, K., Morris, S. (2018) Cycling and spinal trauma: A worrying trend in referrals to a national spine centre. The Surgeon, Vol. 16(4), pp.202–206.
[19] DePasse, J. M., Durand, W., Palumbo, M. A., Daniels, A. H. (2019) Sex- and Sport-Specific Epidemiology of Cervical Spine Injuries Sustained During Sporting Activities. World neurosurgery, Vol. 122, pp.540–545.
[20] Page, P. S., Burkett, D. J., & Brooks, N. P. (2020) Association of helmet use with traumatic brain and cervical spine injuries following bicycle crashes. British Journal of Neurosurgery, Vol. 34(3), pp.276–279.
[21] Amoros, E., Chiron, M., Martin, J. L., Thélot, B., Laumon, B. (2012) Bicycle helmet wearing and the risk of head, face, and neck injury: a French case--control study based on a road trauma registry. Injury prevention, Vol. 18(1), pp.27–32.
[22] Condrea, O. A., Chiru, A., Togănel, G. R., Trusca, D. D. (2020) The Influence of Vehicle Low Impact Velocity over the Helmet Airbag Deployment and Cyclist Injuries. *The 30th SIAR International Congress of Automotive and Transport Engineering*, Springer, 2020, pp.273–280.
[23] Kurt, M., Laksari, K., Kuo, C., Grant, G. A., Camarillo, D. B. (2017) Modeling and optimization of airbag helmets for preventing head injuries in bicycling. Annals of Biomedical Engineering, Vol. 45, pp.1148–1160.
[24] Stigson, H., Rizzi, M., Ydenius, A., Engström, E., Kullgren, A. (2017) Consumer testing of bicycle helmets. *Proceedings of the IRCOBI Conference,* Antwerp, Belgium, 2017, pp.173–181.
[25] Tse, K. M., Holder, D. (2021) A biomechanical evaluation of a novel airbag bicycle helmet concept for traumatic brain injury mitigation. Bioengineering, Vol. 8(11), p.173.
[26] Vives-Torres, C. M., Valdano, M. *et al.* (2023) The effectiveness of cervical airbags in the control of head and neck kinematics. *Proceedings of the IRCOBI Conference*, Cambridge, 2023, pp.85–104.
[27] Asensio-Gil, J. M., Jokubaityte, E., Valdano, M., Oleaga-Ortega, N., Llobet-Cusí, L., Lopez-Valdes, F. (2024) Parametric Study on the Influence of Impact Energy and Inflation Pressure on the Effectiveness of a Cervical Airbag. *Proceedings of the IRCOBI Conference*, Stockholm, 2024.
[28] Asensio-Gil, J. M., Jokubaityte *et al.* (2025) Experimental study on the effectiveness of a cervical airbag in rear and lateral impacts using BioRID-II and PTW dummies. *Proceedings of the IRCOBI Conference*, Vilnius, 2025.
[29] [ISO/TS 18571] Road vehicles — Objective rating metric for non-ambiguous signals, 2024.
[30] Iraeus, J., Lindquist, M. (2016) Development and validation of a generic finite element vehicle buck model for the analysis of driver rib fractures in real life nearside oblique frontal crashes. Accident Analysis & Prevention, Vol. 95, pp.42–56.

[31] Carroll, J., Been, B., Sundmark, H., Burleigh, M., Li, B (2022) A Powered Two-Wheeler Crash Test Dummy. *Proceedings of the IRCOBI Conference, Porto, Portugal*, 2022, pp.114–115.
[32] Takhounts, E. G., Craig, M. J., Moorhouse, K., McFadden, J., Hasija, V. (2013) Development of brain injury criteria (BrIC). Stapp car crash journal, Vol. 57, pp.243–266.
[33] Gabler, L. F., Crandall, J. R., Panzer, M. B. (2018). Development of a second-order system for rapid estimation of maximum brain strain. Annals of Biomedical Engineering, Vol. 47(9), pp.1971–1981.
[34] Nightingale, R. W., Carol Chancey, V. *et. al* (2007). Flexion and extension structural properties and strengths for male cervical spine segments. Journal of Biomechanics, Vol. 40(3), pp.535–542.

VIII. APPENDIX

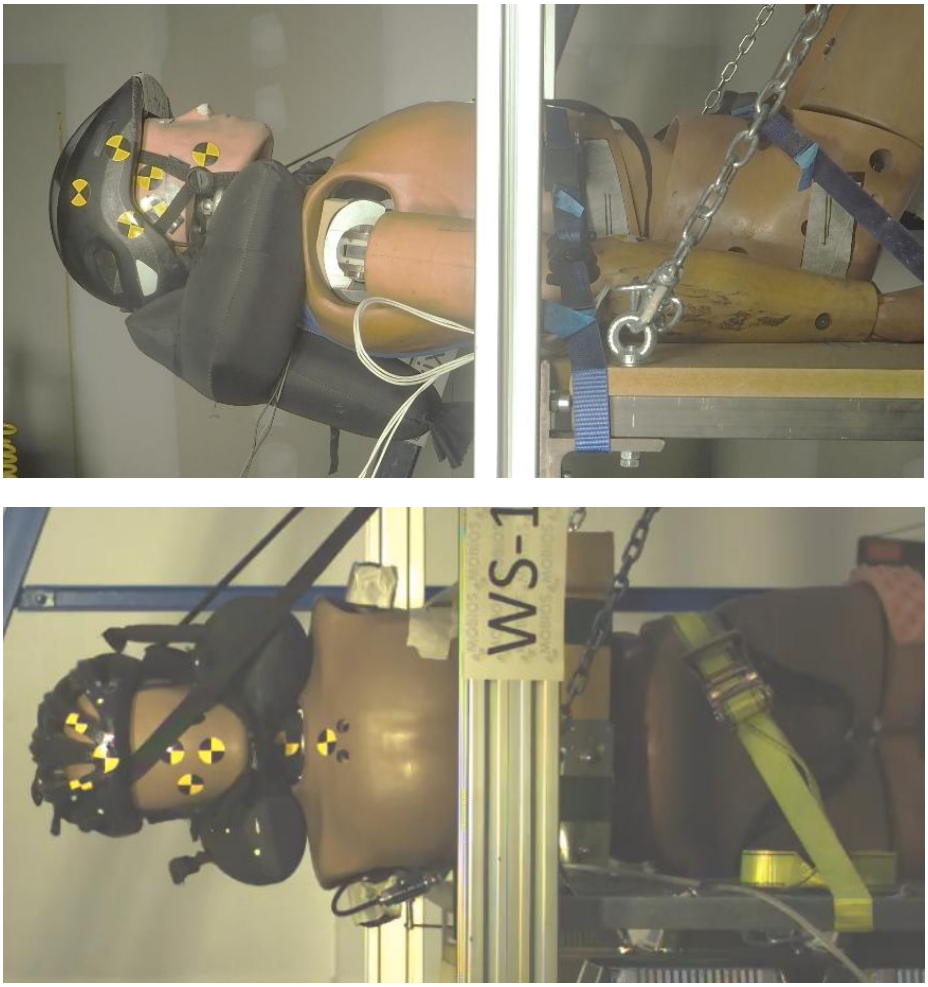

Fig. A1. Experimental test rigs for neck extension (up) and lateral flexion (bottom) cases

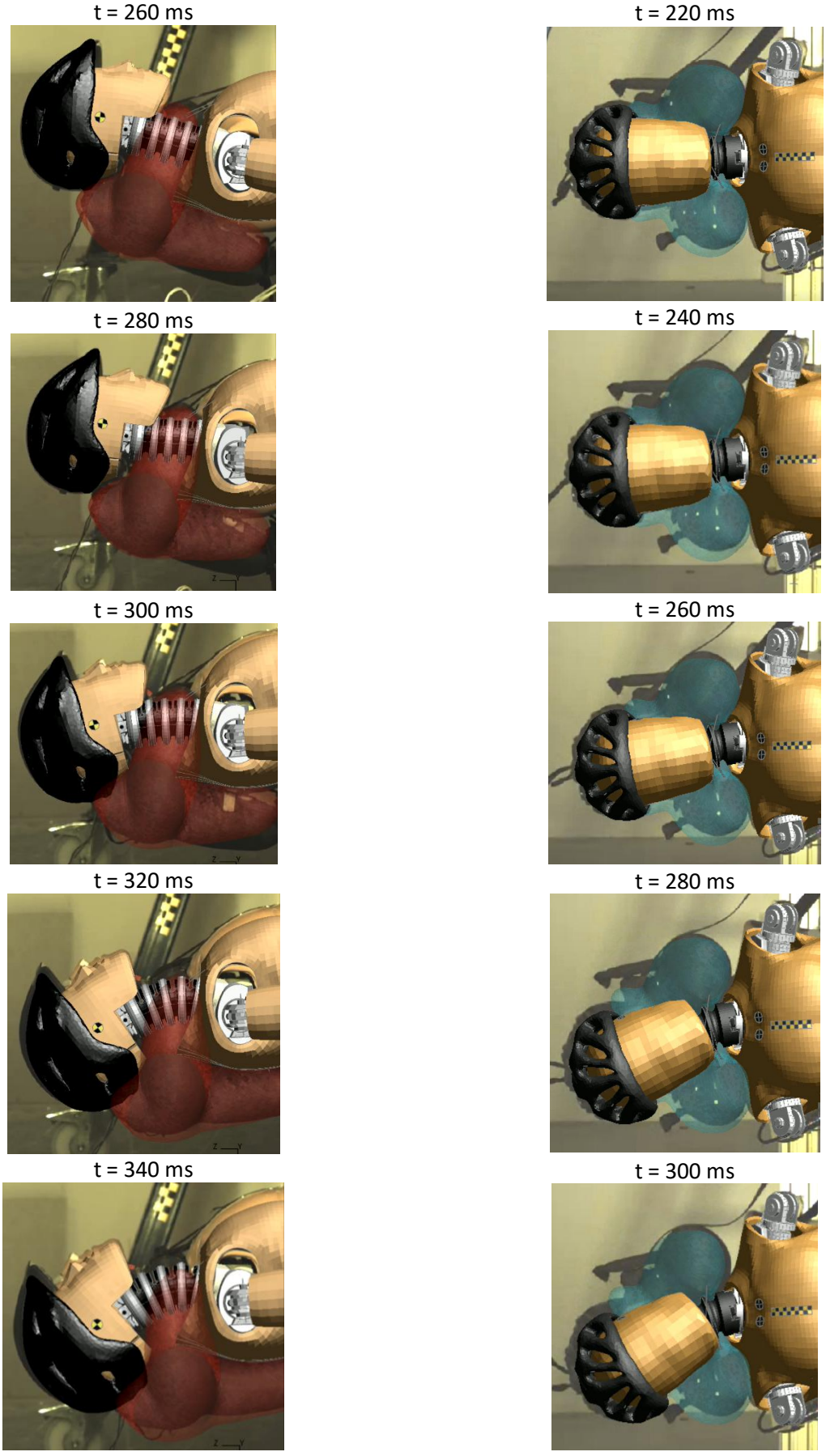

Fig. A2. Simulation versus experiment animation stills from impact initiation to maximum neck extension (left) and flexion (right): Airbag FE model boundary conditions validation based on kinematic behavior agreement between experimental and virtual testing

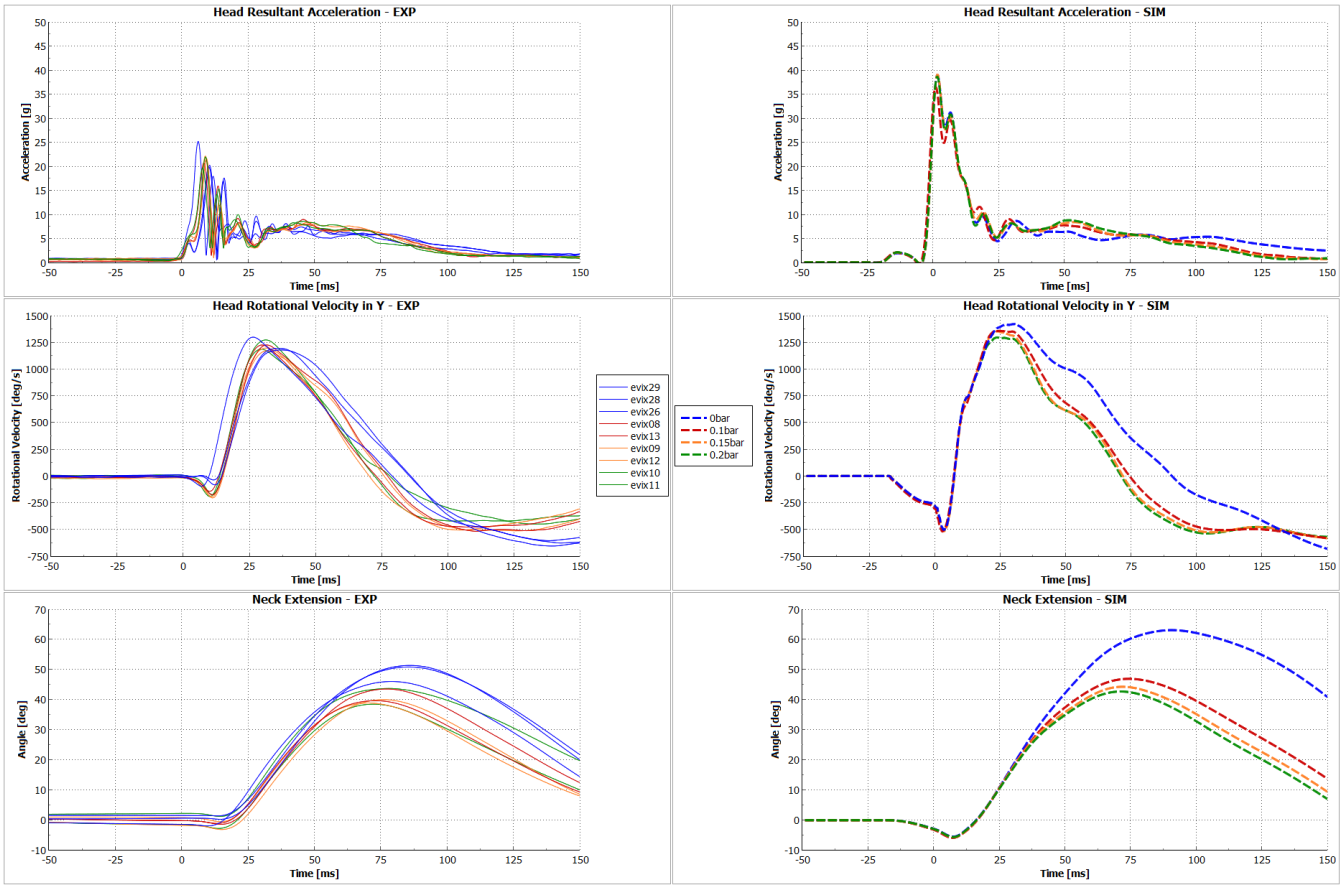

Fig. A3. Experimental (left) and virtual (right) testing data, used for the finite element model validation in neck extension case system

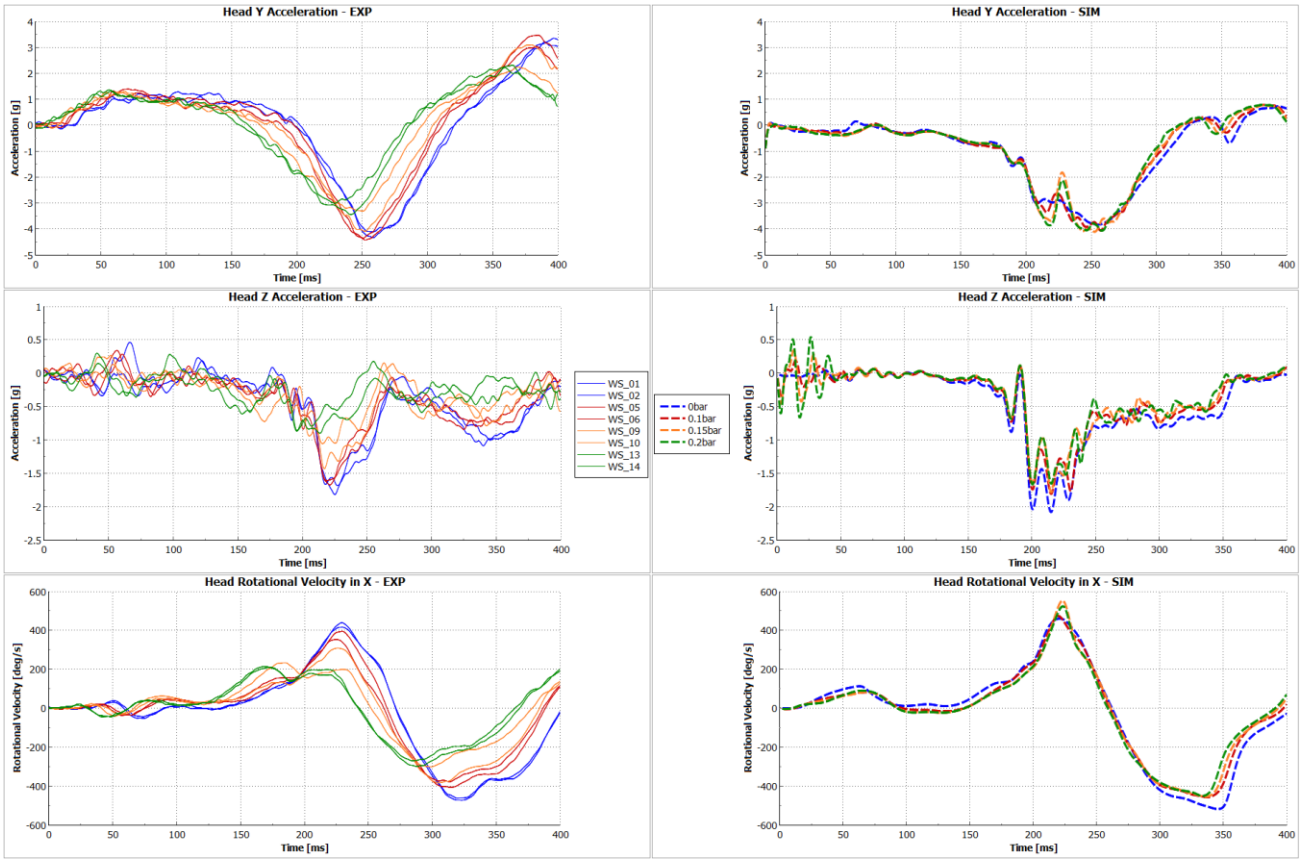

Fig. A4. Experimental (left) and virtual (right) testing head kinematics data, used for the finite element model validation in neck lateral flexion case system for 10 cm falls

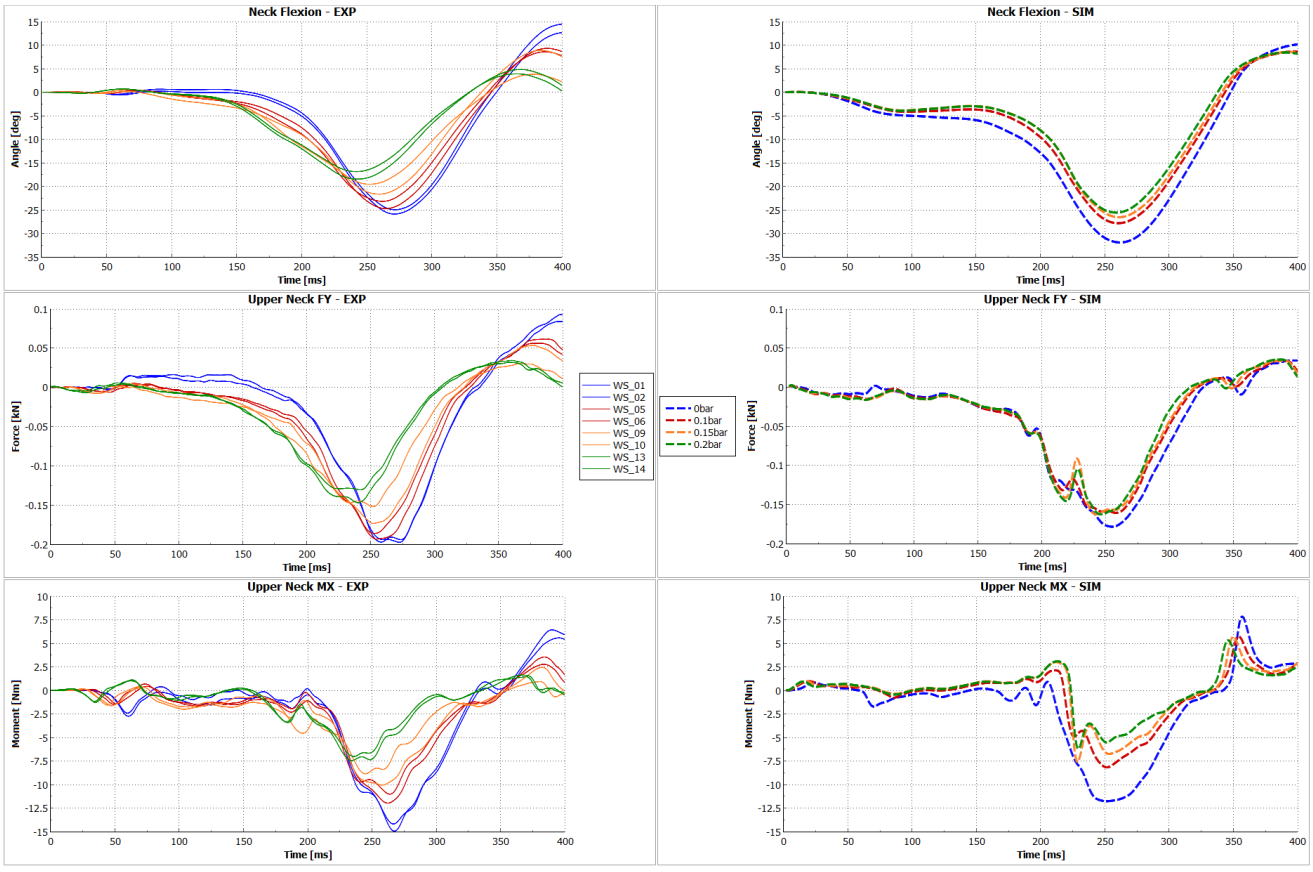

Fig. A5. Experimental (left) and virtual (right) testing neck kinematics and dynamics data, used for the finite element model validation in neck lateral flexion case system for 10 cm falls

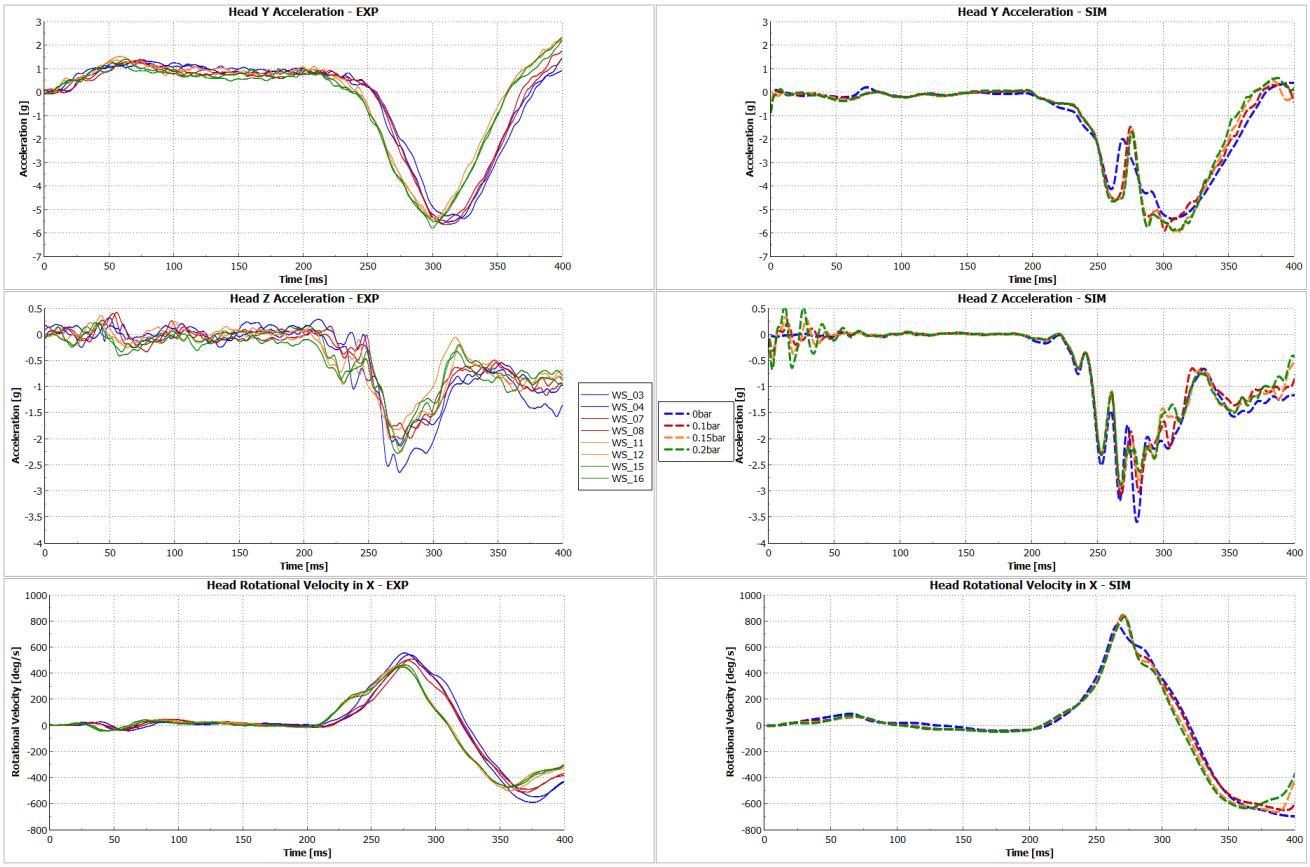

Fig. A6. Experimental (left) and virtual (right) testing head kinematics data, used for the finite element model validation in neck lateral flexion case system for 20 cm falls

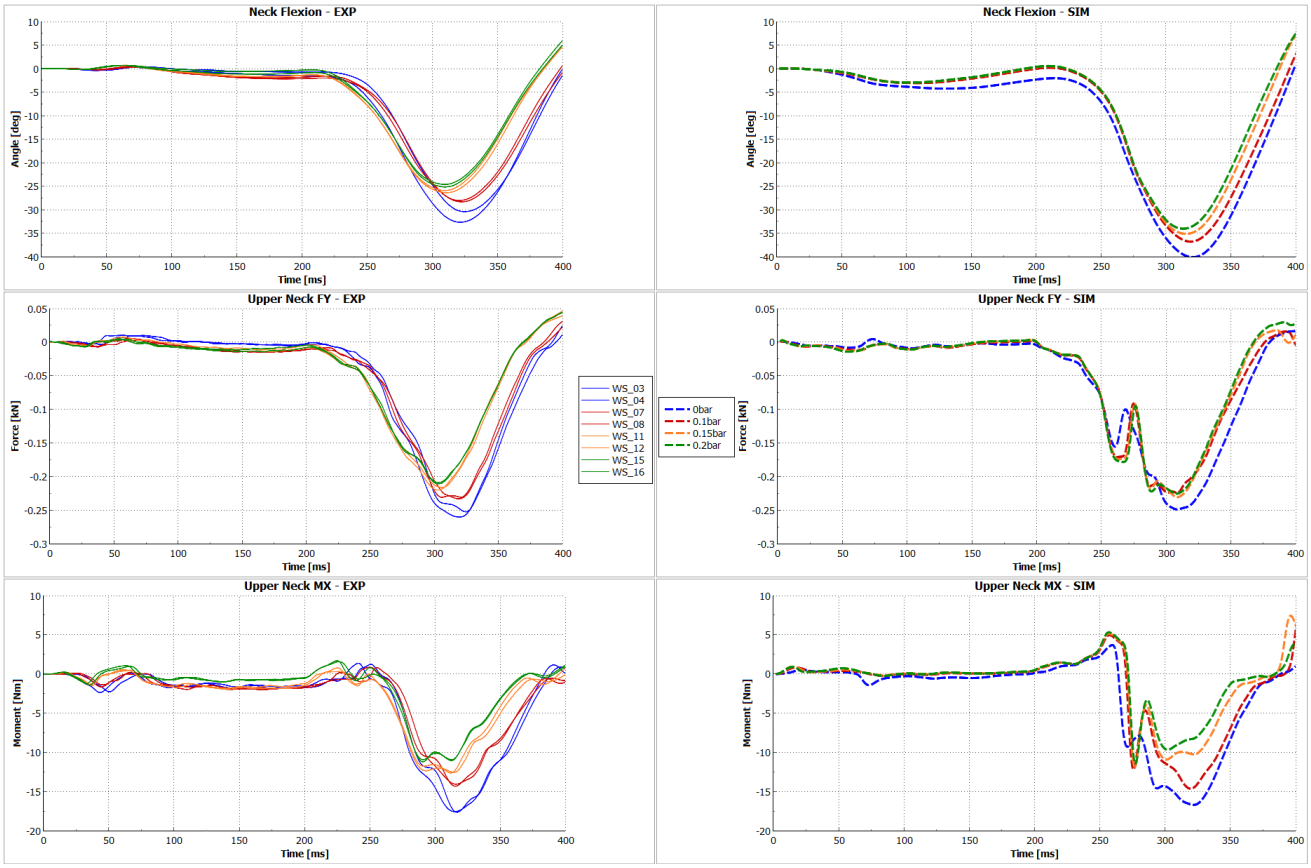

Fig. A7. Experimental (left) and virtual (right) testing neck kinematics and dynamics data, used for the finite element model validation in neck lateral flexion case system for 20 cm falls

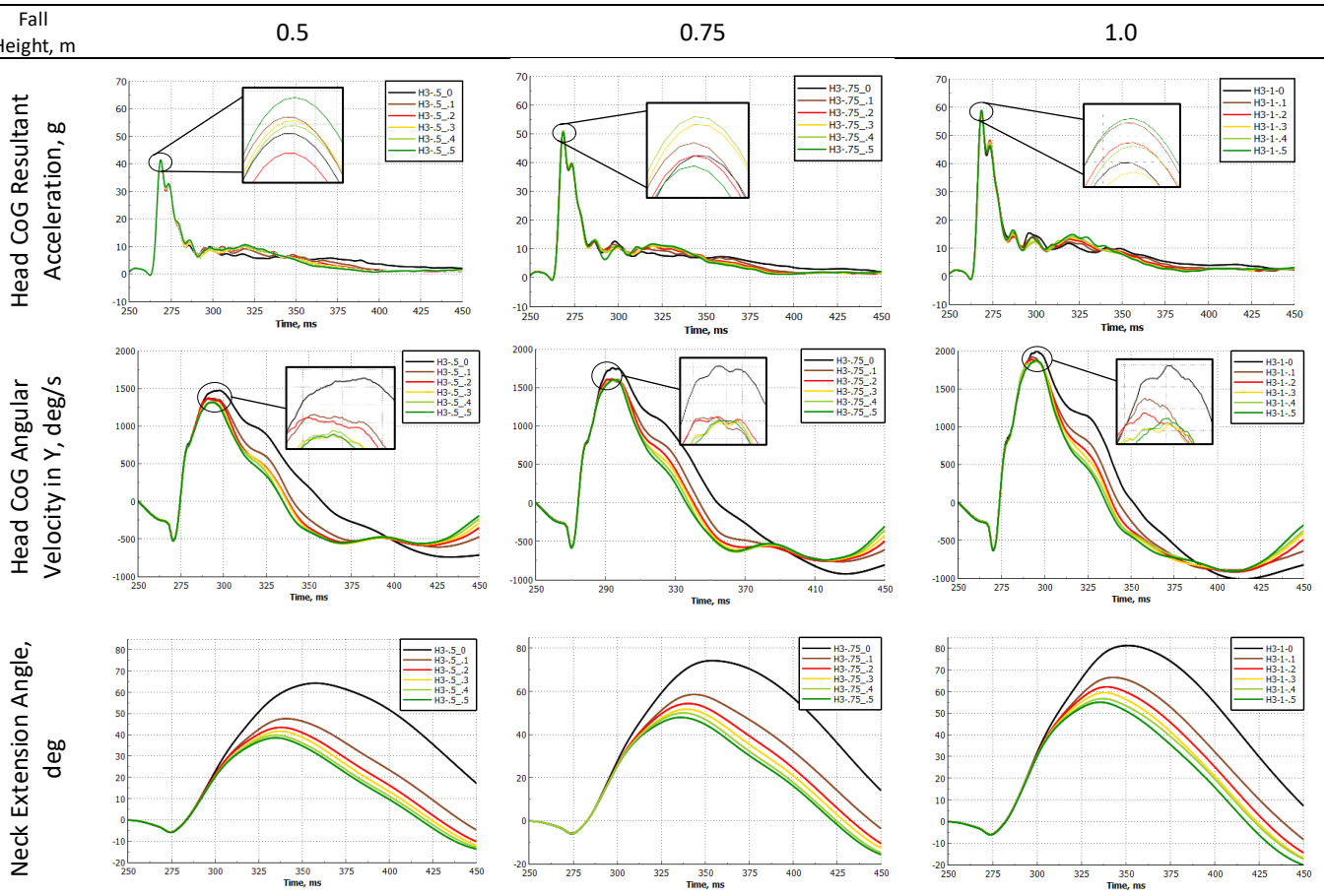

Fig. A8. Simulation responses for neck extension configurations of all fall heights

TABLE AI

ABSOLUTE MAXIMUM PEAK VALUES FOR NECK EXTENSION CONFIGURATION RESPONSES

Signal	Height, m / Pressure, bar	0.5	0.75	1.0
Head CoG Resultant Acceleration, g	0	40.86	50.70	57.99
	0.1	41.11	50.83	58.76
	0.2	40.57	50.71	58.38
	0.3	41.05	51.01	57.81
	0.4	40.98	51.09	58.32
	0.5	41.40	50.60	58.85
Head CoG Angular Velocity, deg/s	0	1475.60	1753.71	1999.15
	0.1	1373.38	1609.94	1923.99
	0.2	1365.07	1610.94	1890.34
	0.3	1315.83	1597.93	1863.15
	0.4	1328.55	1601.99	1867.60
	0.5	1318.68	1600.35	1878.28
Neck Extension Angle, deg	0	64.27	74.23	81.26
	0.1	47.60	58.53	66.55
	0.2	43.47	54.34	62.18
	0.3	41.68	51.70	59.53
	0.4	39.82	50.00	56.73
	0.5	38.56	47.93	55.10

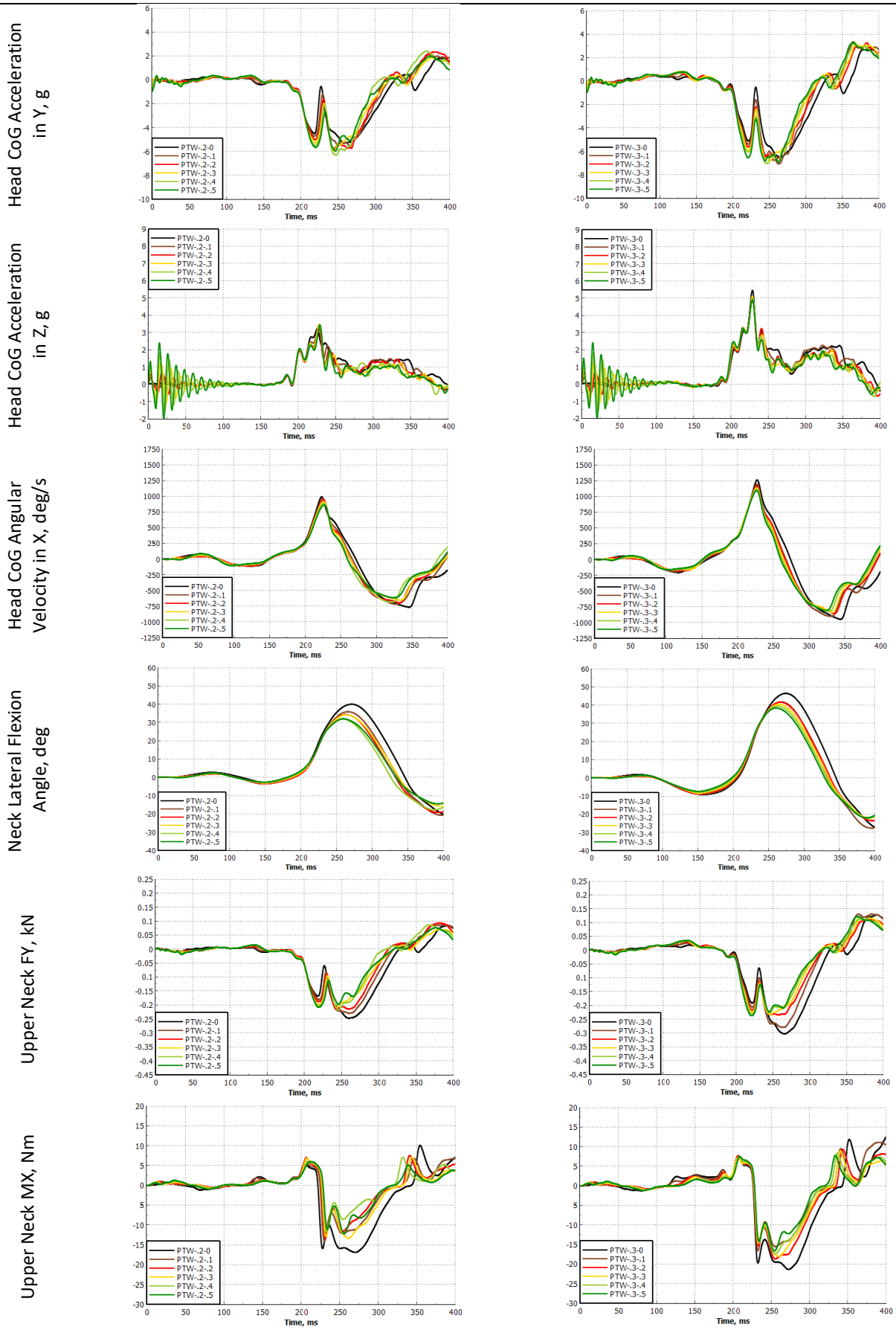

Fig. A9. Simulation responses for neck lateral flexion configurations of 20 cm (left) and 30 cm (right) fall heights

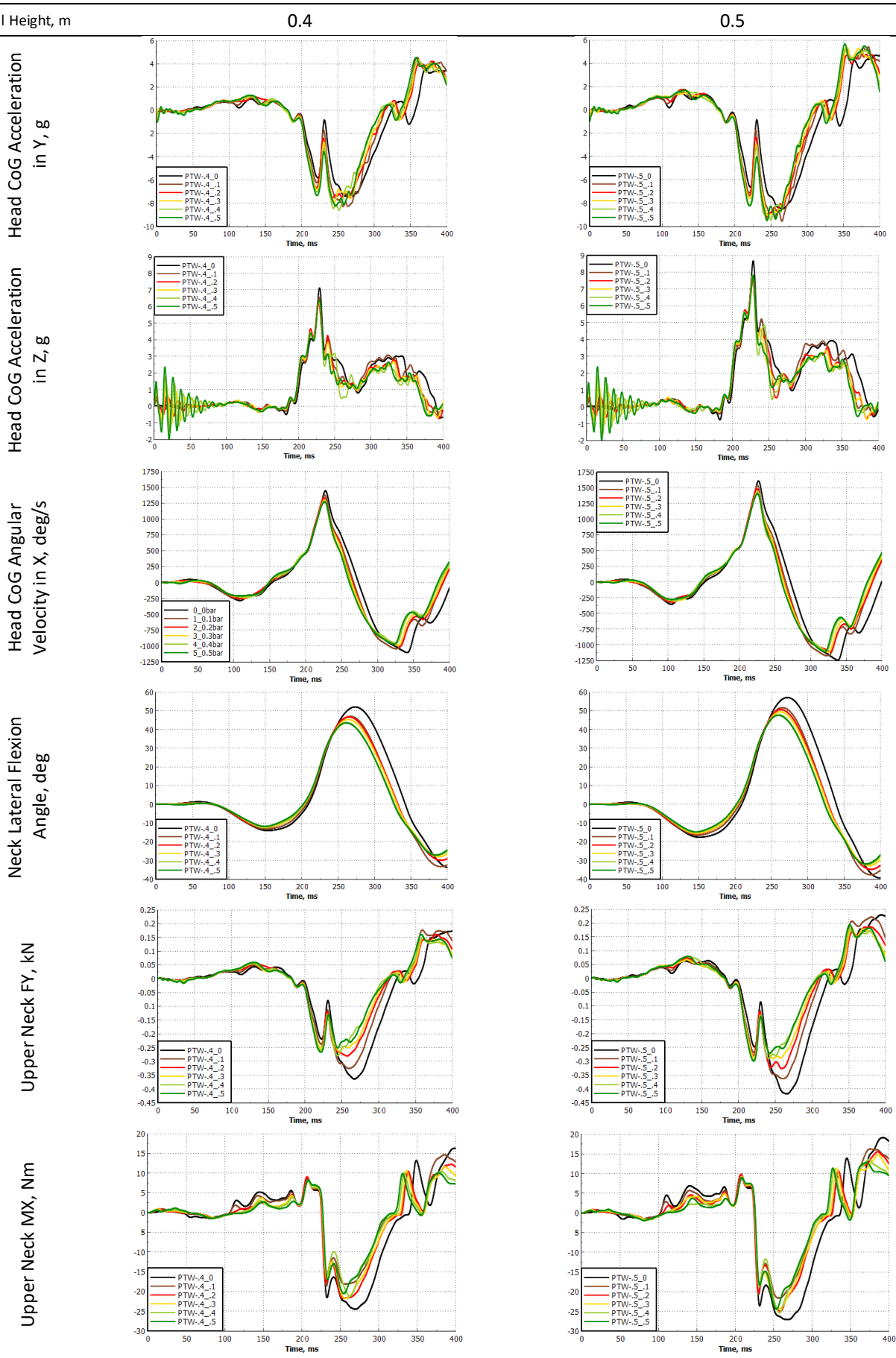

Fig. A10. Simulation responses for neck lateral flexion configurations of 40 cm (left) and 50 cm (right) fall heights

TABLE AIII

ABSOLUTE MAXIMUM PEAK VALUES FOR NECK LATERAL FLEXION CONFIGURATION RESPONSES

Signal	Height, m / Pressure, bar	0.2	0.3	0.4	0.5
Head CoG Acceleration in Y, g	0	5.31	6.49	7.51	8.50
	0.1	5.64	7.08	8.29	9.57
	0.2	5.82	6.63	7.64	9.24
	0.3	6.03	6.85	7.90	9.11
	0.4	6.32	7.06	8.60	9.53
	0.5	5.98	6.91	8.24	9.50
Head CoG Acceleration in Z, g	0	3.21	5.46	7.13	8.68
	0.1	3.37	5.09	6.56	7.80
	0.2	3.44	4.92	6.39	7.68
	0.3	3.48	5.11	6.27	7.80
	0.4	3.36	4.97	6.35	7.80
	0.5	3.44	4.91	6.38	7.82
Head CoG Angular Velocity in X, deg/s	0	989.65	1259.93	1444.32	1608.77
	0.1	963.01	1194.27	1372.45	1533.64
	0.2	946.36	1163.21	1333.73	1482.47
	0.3	917.85	1136.12	1299.88	1440.93
	0.4	888.93	1110.35	1277.97	1431.66
	0.5	859.95	1090.29	1271.10	1401.74
Neck Lateral Flexion Angle, deg	0	39.97	46.46	51.98	57.02
	0.1	35.83	41.73	46.99	51.65
	0.2	34.28	41.60	46.66	50.63
	0.3	34.16	40.44	45.29	49.43
	0.4	31.81	39.44	43.59	47.92
	0.5	32.02	38.36	43.50	47.55
Upper Neck FY, kN	0	0.2474	0.3032	0.3642	0.4182
	0.1	0.2297	0.2798	0.3256	0.3620
	0.2	0.2160	0.2348	0.2808	0.3272
	0.3	0.2091	0.2340	0.2629	0.2908
	0.4	0.2181	0.2301	0.2794	0.2960
	0.5	0.2086	0.2376	0.2668	0.2999
Upper Neck MX, Nm	0	16.91	21.39	24.49	27.11
	0.1	14.17	16.60	18.64	21.64
	0.2	13.41	18.71	21.81	25.06
	0.3	13.39	18.03	21.75	24.40
	0.4	11.64	17.41	21.21	25.39
	0.5	12.22	16.68	20.56	24.45